JOURNAL OF SOLID STATE CHEMISTRY **133,** 104–112 (1997)
ARTICLE NO. SC977324

Epitaxial Growth of Rhombohedral Boron Phosphide Single Crystalline Films by Chemical Vapor Deposition

Y. Kumashiro, H. Yoshizawa, and T. Yokoyama

Faculty of Engineering, Yokohama National University, 156 Tokiwadai, Hodogaya, Yokohama 240, Japan

Received January 16, 1997; accepted February 6, 1997

Rhombohedral boron phosphide ($B_{12}P_2$) single crystalline films were grown at 1100°C by thermal decomposition of a B_2H_6–PH_3–H_2 gas mixture. The crystal quality and orientation of the films, determined by reflection high-energy electron diffraction and X-ray diffraction, are strongly influenced by the flow rates of reactant gases. The epitaxial relationships are $B_{12}P_2$ $(11\bar{2}0)[0001] \parallel$ Si (100)[010], [011] and $B_{12}P_2$ $(10\bar{1}1)[1\bar{2}10]$, $[10\bar{1}4] \parallel$ Si (100)[010], of eight- and twofold symmetry, respectively. The distribution of the two planes in the films changes along the growth direction. The epitaxial relationship on the Si (111) surface is $B_{12}P_2$ (1010)[0001] ∥ Si (111)[110]. The $B_{12}P_2$ $(02\bar{2}1)$ plane grows near the substrate, but the existence of the $(10\bar{1}0)$ plane increases during the crystal growth process. The optimum flow rates of B_2H_6 and PH_3 are 30 sccm for the best epitaxy, which occurs for the lowest mismatch. © 1997 Academic Press

INTRODUCTION

The two boron phosphides, boron monophosphide (BP) with a zinc–blende structure and boron subphosphide ($B_{12}P_2$) with a rhombohedral structure, are refractory materials of high hardness and high melting point. Boron monophosphide decomposes into boron subphosphide and phosphorus at 1100°C (1). Rhombohedral boron subphosphide is a wide gap (2) (3.3 eV) insulator.

The structure of rhombohedral boron phosphide is much like that of α-boron, but has two chains of phosphorus atoms lying within the rhombohedron, connected to six B_{12} icosahedra by two-center bonds (Fig. 1). Rhombohedral boron subphosphide melts at 2120 ± 30°C under argon at 10 MPa (3). Crystal growths of $B_{12}P_2$ have been achieved by applying a partial pressure of phosphorus to a liquid boron–palladium alloy (4, 5) and by chemical vapor deposition (CVD) (6, 7). The former crystals were small in size and did not exhibit crystalline facets. Epitaxial growth by the CVD process is the best method of obtaining high-purity thick wafers. Typical growth of $B_{12}P_2$ by the CVD process is produced either by thermal reduction (5) of a BCl_3–PCl_3 mixture with hydrogen or by thermal decomposition (6, 7) of a B_2H_6–PH_3 mixture with hydrogen. Aselage (5) prepared highly ordered thin films of $B_{12}P_2$ on a Si (100) plane by the former method. Shono *et al.* (6, 7) prepared single crystalline films of $B_{12}P_2$ on Si (100), (110), and (111) surfaces by the latter method.

We have succeeded in preparing semiconducting boron subphosphide wafers (8) on autodoped Si ($\sim 10^{21}$ Si atoms/cm^3) using the CVD process of the B_2H_6–PH_3 system (6) on Si (100) planes. However, X-ray transmission Laue patterns indicated polycrystalline and textured structures. Thus, the growth of single crystalline $B_{12}P_2$ film is needed to prepare well-characterized single crystal wafers for the development of a new refractory semiconductor.

The present paper describes a systematic study of the growth of single crystalline $B_{12}P_2$ films in the B_2H_6–PH_3–H_2 CVD system. Optimum growth conditions are determined by reflection high-energy electron diffraction (RHEED) and X-ray diffraction patterns. As a result, there are two epitaxial relationships on a Si (100) surface, i.e., $B_{12}P_2$ $(11\bar{2}0)[0001] \parallel$ Si (100)[010], [011] and $B_{12}P_2$ $(10\bar{1}1)[1\bar{2}10]$, $[10\bar{1}4] \parallel$ Si (100)[010], influenced by the substrate position, upstream or downstream in the chamber. Furthermore, the distribution of the two planes changes along the growth direction, but the best epitaxy tends to occur under optimum gas flow rates for the lowest mismatch system, $B_{12}P_2$ $(11\bar{2}0) \parallel$ Si (100). In the case of Si (111) substrate, the presence of the $(10\bar{1}0)$ plane increases during the crystal growth process.

EXPERIMENTAL

The horizontal CVD apparatus was the same as that described in our previous report on BP (9) and in the Takigawa *et al.* study (6). The reaction chamber was made of fused quartz with its upper part cooled by running water. Two slopes (9) were placed in front of and to the rear of the SiC-coated graphite susceptor, which removed the vortex flow at the susceptor, giving a more uniform temperature at the substrate. The susceptor was heated externally by an RF generator, and the substrate temperature was measured

0022-4596/97 $25.00

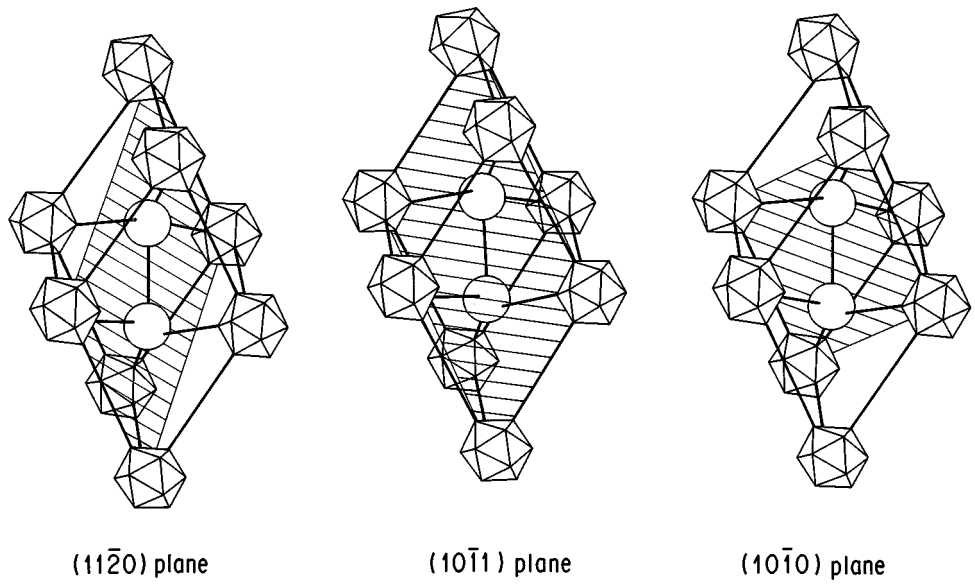

FIG. 1. Crystal structure of $B_{12}P_2$ with a chain composed of two phosphorus atoms joining the boron icosahedra. The circles denote phosphorus atoms. The P atoms of the (11$\bar{2}$0) and (10$\bar{1}$0) surface unit are located in planes. In the case of the (10$\bar{1}$1) surface one P atom (white circle) is above the plane and the other P atom (striped circle) is below the plane.

with an optical pyrometer. $B_{12}P_2$ layers were grown on (100) and (111) oriented p-type Si substrates at $\sim 1\,\Omega\cdot$cm. Research-grade diborane and phosphine diluted to 1 and 5% in hydrogen, respectively, were used as reactant gases. Prior to deposition, the susceptor was heated in hydrogen for 10 min at 1100°C, and then the Si substrate (28×48 mm^2) was heated for 3 min at 1100°C. To determine the optimum gas flow rates for obtaining $B_{12}P_2$ single crystalline films, the films were grown at flow rates of 20–90, 20–100, and 2500 sccm for diborane, phosphine, and hydrogen, respectively. The temperatures 1050 and 1100°C were investigated with reference to the Takigawa *et al.* report (6) and to our previous results (10) with BP epitaxial films. These values were chosen because a decrease in the PH_3 flow rates to lower values or an increase in the growth temperature above 1100°C reduces the phosphorus in BP, giving $B_{12}P_2$.

The growth rate of each film was measured by scanning electron microscope (SEM) observation of a cleaved cross section. The crystallinity of the grown layer was evaluated by X-ray diffraction and RHEED patterns. The RHEED study was carried out after each growth at 20 keV. A SIMS analysis of the film indicates that the majority is silicon ($\sim 10^{21}$ Si atoms/cm^3). Other impurities (Na, K, Ca, and Sn) are present at concentrations on the order of 10^{15} atoms/cm^3.

RESULTS

A. Epitaxial Growth on Si (100)

X-ray diffraction patterns of the films grown on Si (100) surfaces at 1050°C under flow rates of diborane and phosphine of 50/30 and 30/30 sccm, respectively, showed single-phase $B_{12}P_2$ only. RHEED patterns for flow rates of 30 sccm exhibit only $B_{12}P_2$ patterns (Fig. 2). Substrate surfaces in the upstream gas flow (Fig. 2a) show (11$\bar{2}$0) oriented fiber structures, while surfaces in the downstream flow (Fig. 2b) exhibit textured and relatively polycrystalline structures. Growth conditions at 1100°C are listed in Table 1.

X-ray diffraction patterns of the films show $B_{12}P_2$ (Fig. 3). The patterns of films 1, 3, 4, and 7 are rather similar. The common feature of the strongest peak of $(h\,k\,l) = (10\bar{1})$ is characteristic, and peaks from (202), (303), and (404) are found, indicating a (1011) oriented surface. However, other peaks from (110), (200), and (211) are also observed, indicating the possibility of a (11$\bar{2}$0) oriented surface. In the case of film 2 the strongest peak is replaced by a (110) plane accompanying a (220) plane so that the (1120) orientation rather than the (10$\bar{1}$1) predominates. Each peak in films 5 and 6 is

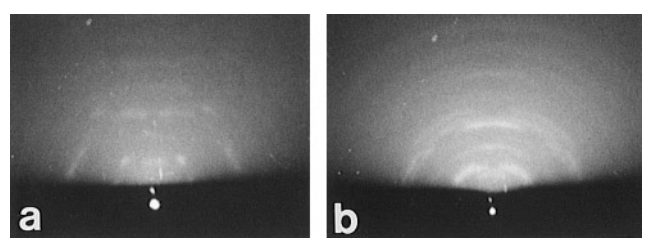

FIG. 2. RHEED patterns from a $B_{12}P_2$ layer grown on a Si (100) surface at 1050°C. (a) Upstream location. (b) Downstream part of the substrate.

TABLE 1
Growth Conditions for $B_{12}P_2$ on Si Substrates at 1100°C

Specimen no.	Substrate	Flow rate of gases PH_3–B_2H_6–H_2 (sccm)	Molecular ratio to H_2		Thickness (μm)	Growth rate (Å/sec)
			B_2H_6	PH_3		
1	Si (100)	30/100/2500	1.2×10^{-4}	2.0×10^{-3}	1.7	4.7
2	Si (100)	30/50/2500	1.2×10^{-4}	1.0×10^{-3}	2.5	6.5
3	Si (100)	30/30/2500	1.2×10^{-4}	6.0×10^{-4}	2.9	7.8
4	Si (100)	50/30/2500	2.0×10^{-4}	6.0×10^{-4}	3.4	10
5	Si (100)	90/30/2500	3.6×10^{-4}	6.0×10^{-4}	3.2	18
6	Si (100)	90/90/2500	3.6×10^{-4}	1.8×10^{-3}	3.8	18
7	Si (100)	20/20/2500	8.0×10^{-5}	4.0×10^{-4}	2.4	5.0
8	Si (111)	30/100/2500	1.2×10^{-4}	2.0×10^{-3}	6.7	7.7
9	Si (111)	30/30/2500	1.2×10^{-4}	6.0×10^{-4}	2.2	8.0
10	Si (111)	50/30/2500	2.0×10^{-4}	6.0×10^{-4}	3.5	14

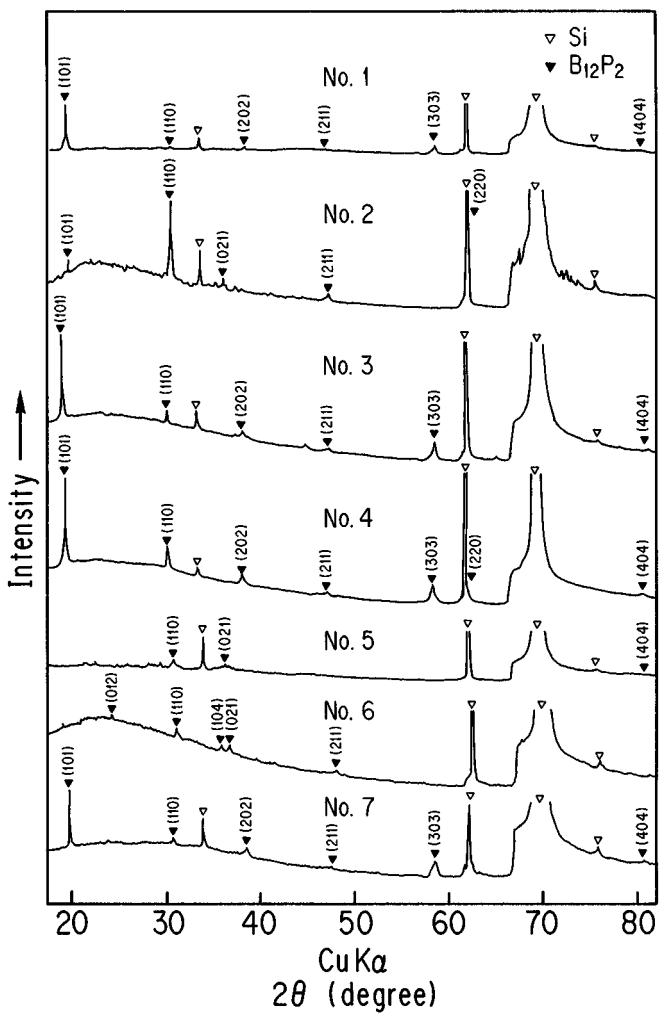

FIG. 3. X-ray diffraction patterns from $B_{12}P_2$ films on a Si (100) surface grown at 1100°C under the growth conditions given in Table 1.

very small, showing poor crystal quality, but the (110) peak appears distinctly oriented to the $(11\bar{2}0)$ surface. Film 6 has many peaks in addition to (110).

The RHEED patterns of film 1 are shown in Fig. 4. Figure 4a with the incident electron beam direction of [011] shows twofold symmetry, which is the twinning pattern of the $B_{12}P_2$ $(10\bar{1}0)$ surface. As $B_{12}P_2$ $(10\bar{1}1)$ has twofold symmetry, directions parallel to Si [011] have $[1\bar{2}10]$ and $[10\bar{1}4]$ directions in the $B_{12}P_2$ $(10\bar{1}1)$ plane. The difference in the patterns of the $[1\bar{2}10]$ and $[10\bar{1}4]$ directions is 90°, but the patterns from these two directions appear simultaneously in Fig. 4. The indexed reflection pattern of the $B_{12}P_2$ $(10\bar{1}1)$ plane, shown in Fig. 5, exhibits extensive twinning. It consists of two kinds of orientation rotated 90° in the $(10\bar{1}1)$ plane, which is confirmed by the fact that rotating Fig. 4a by 34.7° in the $(10\bar{1}1)$ plane results in Fig. 4b. Thus, the epitaxial relationship is $B_{12}P_2$ $(10\bar{1}1)$ $[1\bar{2}10], [10\bar{1}4] \parallel$ Si (100)[011] (Fig. 5).

When the flow rate of phosphine is decreased to 50 sccm (film 2), the RHEED pattern is unclear and the orientation of the film cannot be clarified. However, a further decrease

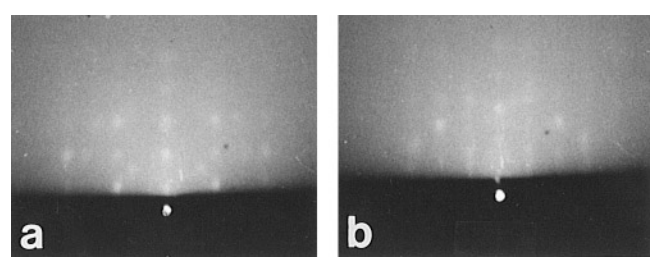

FIG. 4. RHEED patterns from a $B_{12}P_2$ layer of film 1. (a) The incident electron beam direction of [011]. (b) The rotation of (a) by 34.7° in the $(10\bar{1}1)$.

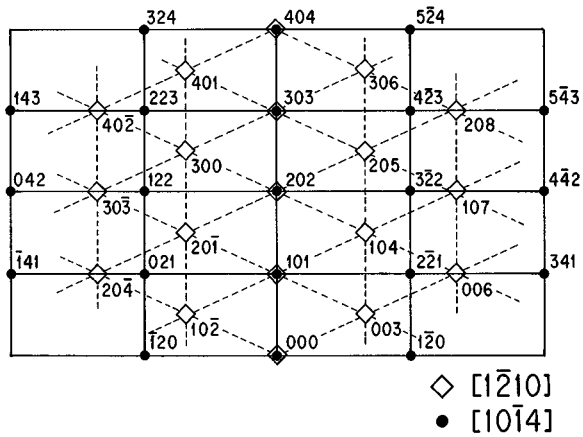

FIG. 5. The indexed reflection patterns from a $B_{12}P_2$ (10$\bar{1}$1) surface.

in the flow rate of phosphine produces clear RHEED spot patterns (film 3). RHEED patterns from the substrate downstream indicate a $B_{12}P_2$ (10$\bar{1}$1) surface (Fig. 4) and a $B_{12}P_2$ (11$\bar{2}$0) surface (Figs. 6a and 6b). The crystal quality of the (11$\bar{2}$0) surface is higher than that of the (10$\bar{1}$1) surface, but the epitaxial relationship between substrate and film is not clear. Figure 6a is a pattern with the incident electron beam in the [0001] direction, and Fig. 6b shows a pattern with the incident electron beam rotating 40.89° from the [0001] direction in the $B_{12}P_2$ (11$\bar{2}$0) plane. Two patterns do not appear regularly when the electron beam incident direction is changed. The RHEED patterns from the upstream position of the substrate indicate a $B_{12}P_2$ (11$\bar{2}$0) surface (Figs. 6c–6e). In contrast, the patterns from the upstream part of the gas flow in Figs. 6c–6e represent eightfold symmetry of the (11$\bar{2}$0) plane. The indexed reflection patterns of the $B_{12}P_2$ (11$\bar{2}$0) plane are shown in Fig. 7. Figure 6c corresponds to $B_{12}P_2$ (11$\bar{2}$0)[0001] when incident along the Si [011] and [010] directions. The pattern of Fig. 6d corresponds to the [1$\bar{1}$01] direction by further rotation by 60° with respect to Fig. 6c. Rotating 23.41° with respect to Fig. 6c results in the pattern of Fig. 6e. These results are consistent with the indexed pattern (Fig. 7). The epitaxial relationship $B_{12}P_2$ (11$\bar{2}$0)[0001] ∥ Si (l00)[011], [010] indicates the existence of a twin structure.

Let us consider the crystal quality of the film after the flow rate of diborane is increased under a constant phosphine flow rate of 30 sccm. Film 4 has two different orientations in one substrate, i.e., $B_{12}P_2$ (10$\bar{1}$0) twinning showing twofold symmetry at the downstream gas flow and (11$\bar{2}$0) twinning or fiber structure at the upstream gas flow. The former is the same as film 2. Films 5 and 6 have low crystal quality consisting of (11$\bar{2}$0) oriented fiber and polycrystalline structures. Film 7, whose flow ratio of PH_3 to B_2H_6 is unity, has two different orientations also, which are in reverse relation to film 4, but the crystallinity deteriorates where partial fiber patterns appear. The surface morphology of the films observed by SEM is shown in Fig. 8. Films 1, 2, 5, and 6 have fine crystal grains, while films 3 and 4 have large oriented grains. Film 7 shows plate-like crystal grains, but is similar to film 3.

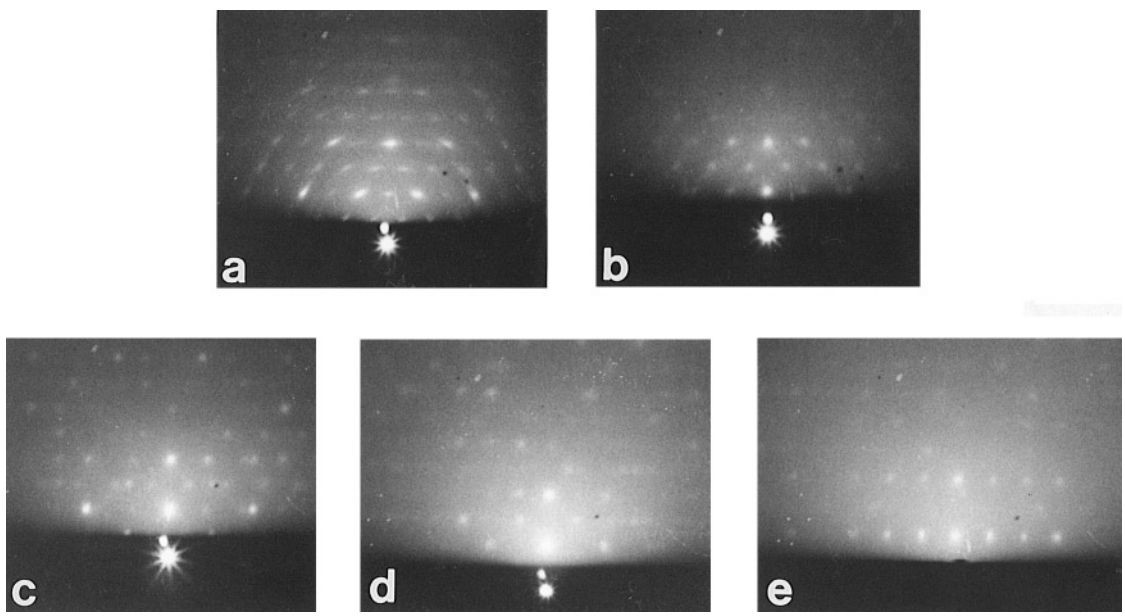

FIG. 6. RHEED patterns from a $B_{12}P_2$ layer of film 3. (a and b) Downstream. (c–e) Upstream region of the substrate.

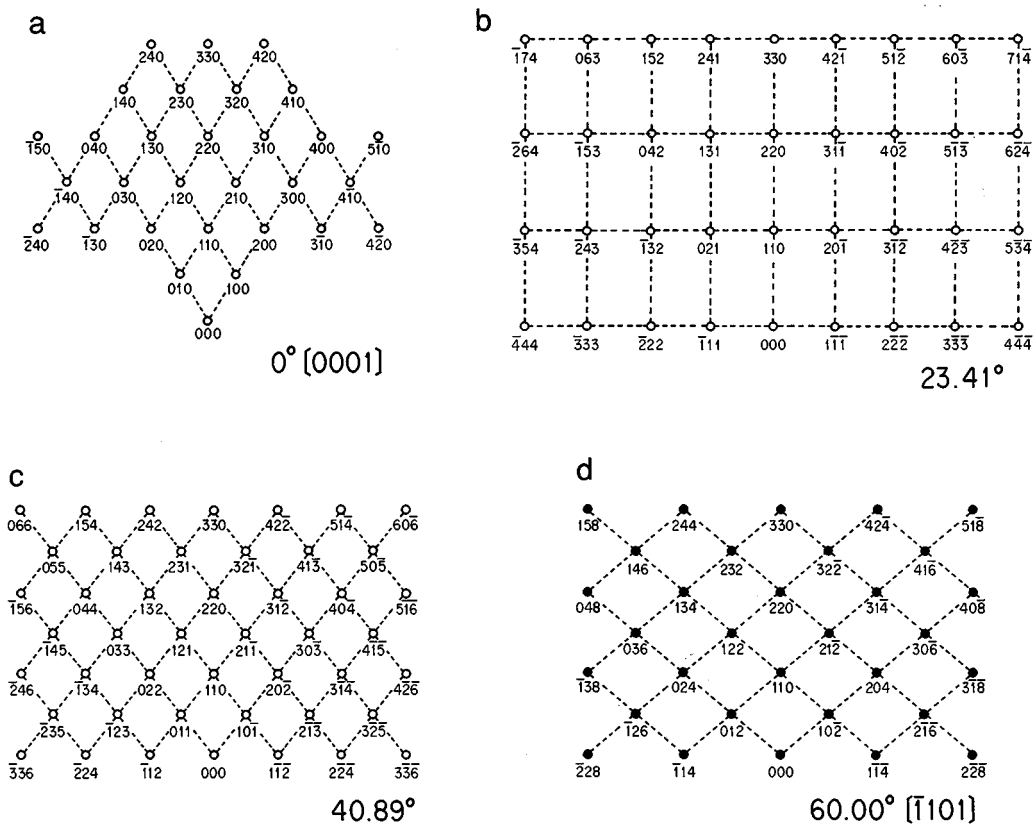

FIG. 7. The indexed RHEED patterns of film $B_{12}P_2$ ($11\bar{2}0$) film.

B. Epitaxial Growth on Si (111)

The X-ray diffraction patterns of the films are shown in Fig. 9. The characteristic features of the Si (111) surface are the existence of SiB_6 and the strong (021) peak accompanying the (300) peak. X-ray diffraction of film 10 indicates many peaks of SiB_6, which is in accord with an increase in the diborane flow rate. The RHEED pattern of film 8 orients to the $B_{12}P_2$ ($11\bar{2}0$) surface, but the RHEED pattern does not appear regularly in accordance with the incident electron beam, so that the relationship between film and substrate is not clear. Films 9 and 10 are epitaxially grown on the $B_{12}P_2$ ($10\bar{1}0$) plane. The RHEED and indexed patterns of film 9 are shown in Figs. 10 and 11. The pattern with the incident electron beam in the [0001] direction appears by incidence of the electron beam in the Si [011] direction, showing formation of a twin. Also, various orientations in the (1010) plane show the relationship $B_{12}P_2$ ($10\bar{1}0$) [0001] ∥ Si (111)[011].

With increasing diborane flow rate under constant phosphine flow rate (film 10), $B_{12}P_2$ (1010)[0001] is observed in various electron beam directions, which indicates that various oriented crystal grains are growing. Polycrystalline rings are also shown. SEM observation of the films (Fig. 8) shows that film 8 has a rough surface with steps, film 9 has the smoothest surface, and film 10 has a characteristic pattern with long and narrow crystal grains parallel to the Si [110] direction. Film 9, characterized by a symmetric RHEED pattern and surface morphology, indicates that similarly oriented grains exist over a wide range.

DISCUSSION

Takigawa *et al.* (6) measured layered growth of $B_{12}P_2$ as a function of substrate temperature under a flow rate of 2500 sccm hydrogen and 50 sccm reactant gases (1% in H_2) of B_2H_6 and PH_3. From 700 to 1050°C, the deposition rate varied exponentially with temperature, in accordance with an Arrhenius expression, and the films were oriented as $B_{12}P_2$ polycrystals. In the region above 1050°C, the deposition rate versus temperature was almost constant, with a value of about 0.1 μm/min, and a single crystal layer of $B_{12}P_2$ was epitaxially grown on Si. Takigawa *et al.* found different orientation between $B_{12}P_2$ and the Si (100) plane (Fig. 1), depending on the flow rates of the reactant gases, i.e., $B_{12}P_2$ ($10\bar{1}1$)[$1\bar{2}10$] ∥ Si (100)[011], $B_{12}P_2$ ($11\bar{2}0$) [0001] ∥ Si (100)⟨010⟩, and $B_{12}P_2$ ($10\bar{1}0$)[0001] ∥ Si (111)[$\bar{1}01$].

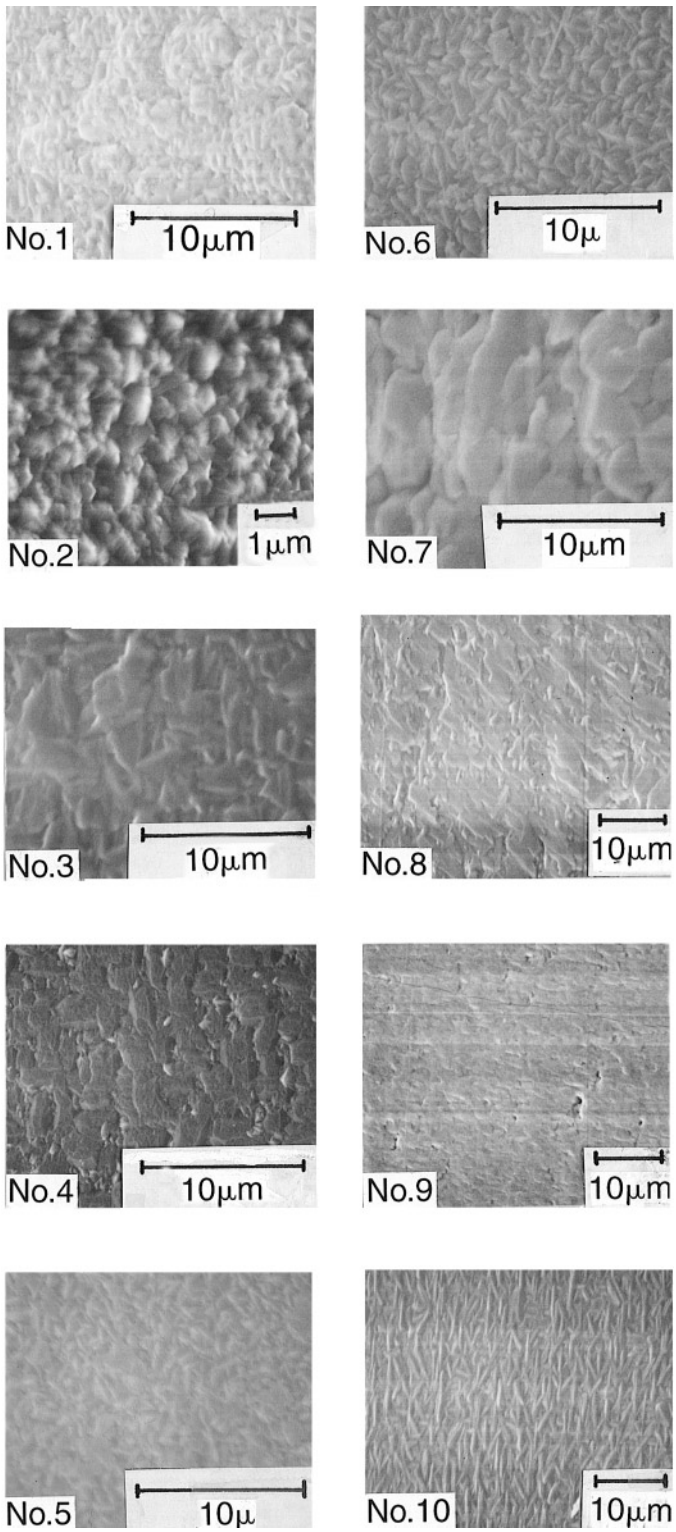

FIG. 8. SEM images of the surface of $B_{12}P_2$ layers (Table 1).

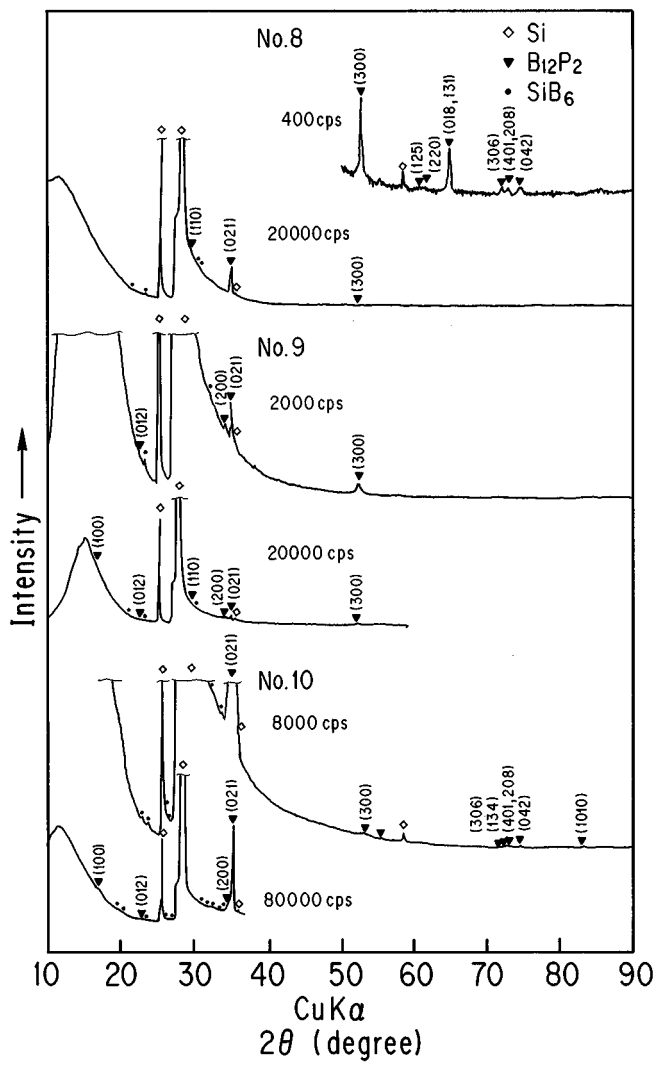

FIG. 9. X-ray diffraction patterns from $B_{12}P_2$ films on Si (111) surfaces under the growth conditions given in Table 1.

In the present case, the growth rate of the film deposited at 1100°C is two times higher than that deposited at 1050°C. The films grown at 1050°C are oriented $B_{12}P_2$ and those at 1100°C are single crystalline $B_{12}P_2$. Therefore, the growth at 1050 and 1100°C corresponds to the low and high temperature regions reported by Takigawa *et al.* (6), respectively.

In a diffusion-limited process (9), mass transport through the stagnant layer cannot compete with the surface reaction. Consequently, deposition will take place preferentially at surface irregularities in the diffusion-limited process, leading to a rough surface. In reaction-limited processes (9), CVD layers with uniform thickness are obtained, provided that the reaction rate over the substrate surface is site-invariant. The above experimental results and SEM observations (Fig. 8) suggest that the deposition at 1100°C is limited by the diffusion process of the reactant gases under a hydrogen atmosphere.

Takigawa *et al.* (6) confirmed that the crystal quality of the films is not essentially influenced by the flow ratio of phosphine to diborane, but is determined by the flow rate

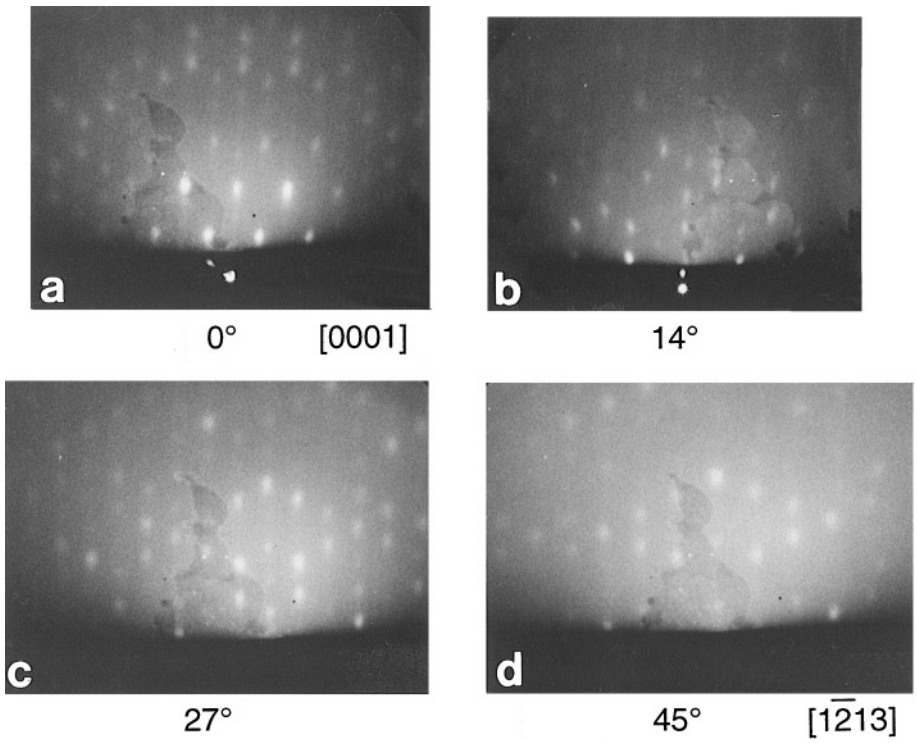

FIG. 10. RHEED patterns from a $B_{12}P_2$ layer of film 9.

ratio of the reactant gases to the hydrogen carrier when the molecular ratio of diborane and phosphine to hydrogen is lower than 3.2×10^{-4}. This is in conflict with the general experimental results of Goossens (12) who used different molar gas ratios of diborane to phosphine (10) for the deposition of B_xP films on various substrates.

The present results indicate that the flow of the reactant gases is the most important parameter determining the crystal quality, surface morphology, and growth rate and that there are optimum flow rates of the reactant gases for good crystal quality.

When we consider the structure of icosahedral boron phosphide ($B_{12}P_2$) (Fig. 1), the $(10\bar{1}0)$ and $(11\bar{2}0)$ surfaces of $B_{12}P_2$ consist of both boron icosahedra and phosphorus chains, while the $(10\bar{1}0)$ plane is the face of the rhombohedral unit cell and contains only icosahedra. The atomic misfit P in a particular direction is calculated by the formula (6)

$$P = (n \times i_{A\langle h\,k\,l\rangle} - m \times j_{B\langle h'\,k'\,l'\rangle})/n \times i_{A\langle h\,k\,l\rangle},$$

where $i_{A\langle h\,k\,l\rangle}$ is the repeat distance in the given direction of material A, $j_{B\langle h'\,k'\,l'\rangle}$ is the corresponding distance in material B, and n and m are integers. The atomic misfit is shown in Table 2. The lattice mismatch is relatively large.

The experimental results indicate that $B_{12}P_2$ $(11\bar{2}0)$ and $(10\bar{1}1)$ films grow epitaxially on a Si (100) surface and the relative amounts of the two surfaces depend on the gas flow rates. The distribution of the two surfaces is also influenced by the location on the substrate, whether upstream or downstream. However, the orientation of the film as determined from the X-ray diffraction pattern does not always coincide with that determined from the RHEED pattern, so that the distribution of the two surfaces would change along the growth direction. For film 3 with good crystallinity the strongest peak in the X-ray diffraction pattern and the RHEED pattern belong to the $(10\bar{1}1)$ and $(11\bar{2}0)$ surfaces, respectively, suggesting that the $(10\bar{1}1)$ plane near the surface of the substrate tends to increase the grains oriented along the $(11\bar{2}0)$ plane during crystal growth. Then, the $B_{12}P_2$ $(11\bar{2}0)$ surface would be grown mainly under optimum flow rates of reactant gases because of the lowest mismatch system (Table 2).

$B_{12}P_2$ $(10\bar{1}0)$ films grow epitaxially grown on a Si (111) plane. The strongest X-ray diffraction pattern of $(02\bar{2}1)$ and the RHEED pattern of the $(10\bar{1}0)$ plane for films 9 and 10 indicate that a $(02\bar{2}1)$ film would grow near the substrate and the existence ratio of $(10\bar{1}0)$ grain would increase during the crystal growth process.

Let us consider the cases where the flow rates of the reactant gases deviate from the optimum conditions. First, in the case of less than optimum gas flow rates with a constant flow ratio of phosphine to diborane of unity (film 7), the crystal quality of the film (Fig. 7) deteriorates despite a growth rate lower than that of film 3 (Table 1). This can be

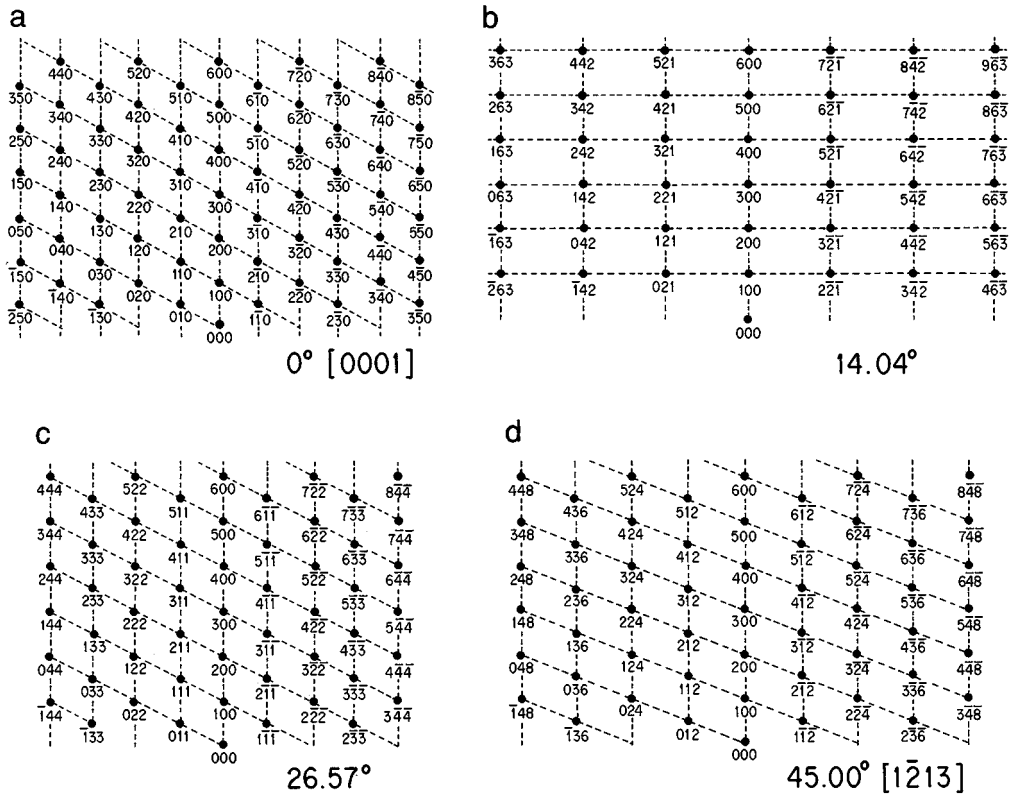

FIG. 11. The indexed reflection patterns from a $B_{12}P_2$ (10$\bar{1}$0) surface.

explained by RHEED observations that the lattice mismatch system of $B_{12}P_2$ (10$\bar{1}$1) ‖ Si (100), is higher than that of $B_{12}P_2$ (11$\bar{2}$0) ‖ Si (100) and would thus predominate. Film 9, with higher than optimal gas flow rates, would result in a high growth rate of 18 Å/sec, causing the crystallinity of the film to deteriorate.

Second, when the flow rate of phosphine is increased at a constant diborane flow rate of 30 sccm, crystal quality deteriorates, as shown in the RHEED and X-ray diffraction patterns. Films 2 and 8 show a transition region, where the orientation of the film is not clear in the former and unexpected orientation of the film, i.e., $B_{12}P_2$ (11$\bar{2}$0) ‖ Si (111), is observed in the latter. Ohsawa *et al.* (13) confirmed by ion microanalysis that autodoping of Si, the substrate, in the epitaxial growth of BP in a BCl_3–PCl_3–H_2 system at growth temperature 1100°C was greater for BP on Si (111) than on Si (100). Thus it is likely that at growth at 1100°C a higher autodoping of Si (111) than of Si (100) would form. Additional precipitation of silicon boride at the initial stage of film growth would produce an epitaxial relationship of $B_{12}P_2$ film 35° off with respect to the ⟨110⟩ direction in Si (111), causing the epitaxial relationship $B_{12}P_2$ (11$\bar{2}$0) ‖ Si (111).

TABLE 2
The Atomic Misfit between $B_{12}P_2$ and Si Substrates

$B_{12}P_2$ ‖ Si	Atomic misfit (%)
$B_{12}P_2$ (11$\bar{2}$0)[0001] ‖ Si (100)[010]	9.1
$B_{12}P_2$ (11$\bar{2}$0)[0001] ‖ Si (100)[011]	2.9
$B_{12}P_2$ (10$\bar{1}$1)[1$\bar{2}$10] ‖ Si (100)[010]	10.1
$B_{12}P_2$ (10$\bar{1}$1)[10$\bar{1}$4] ‖ Si (100)[010]	5.3
$B_{12}P_2$ (10$\bar{1}$0)[0001] ‖ Si (111)[110]	2.9

Finally, when the flow rate of diborane is increased at a constant flow rate of phosphine of 30 sccm, the growth rate for the deposit increases in proportion to the flow rate of diborane (Table 1). However, the crystallinity of the film deteriorates where the RHEED pattern does not appear regularly in accordance with the incident electron beam or partial textured, polycrystal, or amorphous RHEED patterns appear, so that various oriented crystal grains would grow. SEM observation also indicates that smooth and large oriented grains over a wide range under optimum conditions become rough surface, plate-like grains, narrow grains, and fine crystal grains in deviating from optimum growth.

Thus it is concluded that optimum growth conditions exist for gas flow rates in balance with flow rates and supply rates of reactant gases.

It should be mentioned that these films look rough and facetted in their SEM images (Fig. 8). This would possibily determine the RHEED patterns and thus mask the bulk orientation. Thus, the condition for obtaining smooth epitaxial films is closely related to the detailed gas flow behavior (14) at each point in the system and to the heat and mass transfer mechanisms (11). We have discussed large variations between the upstream and downstream regions of the substrate, but we cannot determine whether gas-phase precursor depletion or temperature gradients are the cause.

CONCLUSION

We have obtained epitaxial layers of $B_{12}P_2$ on Si (100) and (111) surfaces at 1100°C by thermal decomposition of the B_2H_6–PH_3–H_2 system in a diffusion process of the reactant gases in hydrogen. $B_{12}P_2$ $(11\bar{2}0)$ and $(10\bar{1}1)$ planes are epitaxially grown on the Si (100) plane and the existence ratios and distribution of two surfaces depend on the gas flow rates and the position in the substrate. In the case of the Si (111) surface, $B_{12}P_2$ $(02\bar{2}1)$ films near the surface of the substrate are replaced by $(10\bar{1}0)$ films during crystal growth. These complex epitaxial relations may be due to the complicated icosahedral–rhombohedral $B_{12}P_2$ structure. The best epitaxy, however, occurs for the lowest mismatch system at optimum gas flow rates.

ACKNOWLEDGMENTS

This study was performed through the Iketani Science and Technology Foundation and through Grant-in-Aid for Scientific Research 06805061 from the Ministry of Education.

REFERENCES

1. J. L. Peret, *J. Am. Ceram. Soc.* **47,** 44 (1964).
2. R. A. Burmeister and P. E. Greene, *Bull. Am. Phys. Soc. Ser.* **10,** 1184 (1965).
3. G. E. Slack, T. F. McNelly, and E. A. Taft, *J. Phys. Chem. Solids* **44,** 1009 (1983).
4. G. E. Slack, D. Oliver, and F. Horn, *Phys. Rev. B* **4,** 1714 (1971).
5. T. L. Aselage, *Mater. Res. Soc. Symp. Proc.* **97,** 101 (1987).
6. M. Takigawa, M. Hirayama, and K. Shono, *Jpn. J. Appl. Phys.* **12,** 1504 (1973).
7. T. Takenaka and K. Shono, *Jpn. J. Appl. Phys.* **13,** 1211 (1974).
8. Y. Kumashiro, H. Yoshizawa, and K. Shirai, *Jpn. J. Appl. Phys. Series* **10,** 166 (1994).
9. Y. Kumashiro, Y. Okada, and H. Okumura, *J. Cryst. Growth* **132,** 611 (1993).
10. Y. Kumashiro, Y. Okada, and S. Gonda, *J. Cryst. Growth* **70,** 507 (1984).
11. K. E. Spear, *Pure Appl. Chem.* **54,** 1297 (1982).
12. A. Goossens, "An Electrochemical Study of Silicon/Boron phosphide Heterojunction Photoelectrode," Ph.D. thesis. Technische Univ. Delft, 1991.
13. J. Ohsawa, T. Nishinaga, and S. Uchiyama, *Jpn. J. Appl. Phys.* **17,** 1579 (1978).
14. K. Chen, *J. Cryst. Growth* **70,** 64 (1984).